



Physical Characteristics of von Willebrand Factor Binding with Platelet Glycoprotein Iba Mutants at Residue 233 Causing Various Biological Functions

Masamitsu Nakayama¹ Shinichi Goto¹ Shinya Goto¹ 

¹ Department of Medicine (Cardiology), Tokai University School of Medicine, Isehara, Japan

Address for correspondence Shinya Goto, MD, PhD, Department of Medicine (Cardiology), Tokai University School of Medicine, 143 Shimokasuya, Isehara, Japan (e-mail: sgoto3@mac.com).

TH Open 2022;6:e421–e428.

Abstract

Glycoprotein (GP: HIS¹-PRO²⁶⁵) Iba is a receptor protein expressed on the surface of the platelet. Its N-terminus domain binds with the A1 domain (ASP¹²⁶⁹-PRO¹⁴⁷²) of its ligand protein von Willebrand factor (VWF) and plays a unique role in platelet adhesion under blood flow conditions. Single amino acid substitutions at residue 233 from glycine (G) to alanine (A), aspartic acid (D), or valine (V) are known to cause biochemically distinct functional alterations known as equal, loss, and gain of function, respectively. However, the underlying physical characteristics of VWF binding with GPIba in wild-type and the three mutants exerting different biological functions are unclear. Here, we aimed to test the hypothesis: biological characteristics of macromolecules are influenced by small changes in physical parameters. The position coordinates and velocity vectors of all atoms and water molecules constructing the wild-type and the three mutants of GPIba (G233A, G233D, and G233V) bound with VWF were calculated every 2×10^{-15} seconds using the CHARMM (Chemistry at Harvard Macromolecular Mechanics) force field for 9×10^{-10} seconds. Six salt bridges were detected for longer than 50% of the calculation period for the wild-type model generating noncovalent binding energy of -1096 ± 137.6 kcal/mol. In contrast, only four pairs of salt bridges were observed in G233D mutant with noncovalent binding energy of -865 ± 139 kcal/mol. For G233A and G233V, there were six and five pairs of salt bridges generating -929.8 ± 88.5 and -989.9 ± 94.0 kcal/mol of noncovalent binding energy, respectively. Our molecular dynamic simulation showing a lower probability of salt bridge formation with less noncovalent binding energy in VWF binding with the biologically loss of function G233D mutant of GPIba as compared with wild-type, equal function, and gain of function mutant suggests that biological functions of macromolecules such as GPIba are influenced by their small changes in physical characteristics.

Keywords

- platelet
- von Willebrand factor
- salt bridge
- molecular dynamic

received
May 20, 2022
accepted after revision
August 5, 2022
accepted manuscript online
September 7, 2022

DOI <https://doi.org/10.1055/a-1937-9940>.
ISSN 2512-9465.

© 2022. The Author(s).

This is an open access article published by Thieme under the terms of the Creative Commons Attribution-NonDerivative-NonCommercial-License, permitting copying and reproduction so long as the original work is given appropriate credit. Contents may not be used for commercial purposes, or adapted, remixed, transformed or built upon. (<https://creativecommons.org/licenses/by-nc-nd/4.0/>)

Georg Thieme Verlag KG, Rüdigerstraße 14, 70469 Stuttgart, Germany

Introduction

Platelet adhesion and cohesion under blood flow conditions are mediated exclusively by the A1 domain of von Willebrand factor (VWF) located between the D3 and the A2 domain (residues ASP¹²⁶⁹-PRO^{1472,1,2} 23.87 kDa)³ binding with glycoprotein (GP) Iba, a receptor protein expressed on the surface of platelet, regardless of the activation status of the platelets.^{4–7} Specific binding characteristics of GPIba binding with VWF include transient binding without stabilization in the absence of specific modulators such as ristocetin that was originally developed as antibiotics⁸ but demonstrated to induce VWF-mediated platelet aggregation⁹ or botrocetin which was purified from snake venom to induce VWF-mediated platelet aggregations.^{10–13} Transient platelet adhesion mediated by VWF binding with platelet GPIba could be detected under blood flow conditions,⁴ but the binding is not stable without the contribution of another VWF/fibrinogen receptor of GPIIb/IIIa alternatively named as integrin $\alpha_{IIb}\beta_3$, the function of which is activation dependent¹⁴ on the absence of ristocetin or botrocetin.¹⁵ Transient adhesion and cohesion of platelet under high shear flow condition plays crucial roles in both thrombus formation and haemostasis.^{5,16} Accordingly, the bleeding risk increases in conditions where either the quantity or quality of platelet GPIba and VWF are reduced.

The von Willebrand diseases (VWDs) were primarily characterized as bleeding disorders induced by quantitative or qualitative abnormality of VWF.¹⁷ Since the major functions of A1 domain of VWF in hemostasis and thrombus formation are mediated by its binding with platelet GPIba,^{4,5,18,19} the functional abnormality in GPIba also causes similar conditions: namely platelet type VWD.^{20,21} Mutations in platelet GPIba cause VWD either by reducing (loss of function) or enhancing (gain of function) its abilities to bind with VWF.^{20,22,23} While the loss of function mutant(s) of GPIba causes VWD because the GPIba could not bind with VWF, the gain of function mutant(s) of GPIba causes VWD due to enhanced consumption of larger multimers of VWF by stabilizing GPIba binding with VWF even in the absence of ristocetin.²⁴ Previous biological and crystallographic analysis revealed the importance of C-terminal disulfide loop region (Cys209–Cys248) in GPIba for its binding with VWF.^{25–27} Indeed, both loss of and gain of function of GPIba could be achieved by a single amino acid substitution at G233 in GPIba.^{23,28,29} The biological functions of macromolecules such as VWF binding with GPIba may be influenced by a small change in their physical characteristics.³⁰ Previous biological experiments have shown that GPIba with mutation at residue 233 have a distinct biological phenotype, although the theoretical mechanism is unknown.²³ This makes the G233 mutants as a suitable target for analysis.

The molecular dynamic (MD) simulation is a relatively novel technic for biology. The strength of MD simulation is the ability to clarify the quantitative physical and dynamic characteristics of protein–protein interactions including the binding of GPIba to VWF. Indeed, the binding energy equivalent potential of mean forces (PMFs) and binding force in

GPIba binding with VWF were calculated by MD simulation.³¹ Interlandi et al revealed the importance of salt bridge formation between amino acids located at N-terminal linker in VWF and corresponding N-terminus region in GPIba by MD simulation.³² Previous publications revealed that single amino-acid mutation at residue 233 located in the β -switch in GPIba causes biological loss and gain of function for binding with VWF at various binding energies.^{23,31} However, the salt bridge formation and noncovalent binding energy between VWF and GPIba mutants with various biological functions are still to be elucidated. A previous report described that the dissociation energy of GPIba with loss-of-function mutant from VWF is only slightly lower compared with wild-type. Thus, we hypothesized that the biological functions of macromolecules of VWF and GPIba with various G233 mutants are driven by small changes in their physical characteristics including salt-bridge formation and attempted to test this hypothesis.

Methods

Molecular Dynamic Simulation

Initial Structure of Glycoprotein Iba Binding with von Willebrand factor

The position coordinates and velocity vectors of all the atoms constructing the A1 domain of VWF (VWF: residues ASP (D):1269-PRO(P):1466) binding with the N-terminal domain of platelet GPIba (GPIba: residues HIS(H):1-PRO(P):265) were solved by MD simulation calculation as previously published.^{2,31} The energetically most stable structure with a mass center distance between GPIba and VWF of 27.3 Å was selected as the initial structure of wild-type GPIba bound with VWF. The amino acid G233 at GPIba in this structure was substituted by A, D, and V to provide initial binding structures with VWF.

Molecular Dynamic Simulation Calculation

Water molecules modeled as Chemistry at Harvard Macromolecular Mechanics (CHARMM) transferable intermolecular potential with three interaction sites were placed around the molecules constructing VWF bound with wild-type and G233A, G233D, and G233V mutant GPIba.³³ Then, Newton's second law known as $F \text{ (force)} = M \text{ (mass)} \times A \text{ (acceleration)}$ was solved for all atoms constructing GPIba, VWF, and water molecules around them with multidimensional calculations using Nanoscale Molecular Dynamics (NAMD) software as previously published.^{2,31} The effects of any modulators such as ristocetin were not considered. The calculation was conducted on the computers equipped with four sets of NVIDIA Tesla V100 GPU (HPC5000-XSLGPU4TS, HPC systems Inc., Tokyo, Japan). The CHARMM-36 was used as a governing force field.^{34,35} The position coordinates and velocity vectors of each atom and water molecule were calculated in each 2.0 femtosecond (10^{-15} s). The cut-off length of 12 Å was set as the maximum distance allowing direct interactions of atoms as previously published.² Visual Molecular Dynamics (VMD) version 1.9.3

was used for visualization of the results such as the snap-shot of the three-dimensional structure of VWF binding with GPIba from the position coordinates of atoms constructing VWF and GPIba.^{2,31}

Root Mean Square Deviations

In each calculated structure, the average distances between various atoms excluding water molecules were calculated as the root mean square deviations (RMSDs). The RMSDs were calculated every 10 ns from the beginning to the end of the calculation.

Noncovalent Binding Energy

The noncovalent binding energies between amino acids constructing GPIba and VWF were calculated with VMD and NAMD energy plugin (version 1.4) as described previously.^{30,36–38} The noncovalent binding energy was expressed as kilocalorie per mole.

Salt Bridge Formation

Anionic carboxylate of either aspartic acid (N) or glutamic acid (E) is known to form salt bridges with cationic ammonium (RNH^{3+}) of lysine (K) or the guanidinium ($\text{RNHC}(\text{NH}_2)^{2+}$) of arginine (R).³⁹ Since the salt bridges were formed between positively charged portions and negatively charged ones,⁴⁰ they formed bridges when the distance between these amino acids became less than 4 Å or closer.⁴¹ Within all calculated structures, the presence of salt bridges was calculated by the VMD plug-in software Salt Bridges Plugin (Version 1.1) as previously published.^{42,43} The percentage of the time when the pairs of amino acids form salt bridges within the calculation period was measured.

Statistical Analysis

The calculated results of RMSDs and noncovalent binding energy in each condition are shown as mean \pm standard deviation unless otherwise described. The values in wild-type and each of G233A, G233D, and G233V mutant were compared by using two-tailed Student's *t*-tests. *p*-Values less than 0.05 were considered to denote statistical significance.

Results

Initial Structure and Root Mean Square Deviations

Panel A in ▶Fig. 1 shows the position of G233 in the energetically stable structure of wild-type GPIba bound to VWF. Each picture in panel B shows the initial positions of amino acid at 233 in GPIba in wild-type and the three mutants. The initial binding structure of GPIba and VWF were similar across wild-type and all the mutants.

▶Fig. 2 shows the time-dependent changes in RMSDs of atoms constructing GPIba and VWF excluding water molecules in wild-type and the three mutants. RMSDs stabilized with a fluctuation of less than 3 Å in all conditions within 600 ns of calculation.

Noncovalent Binding Energy between Glycoprotein Iba and von Willebrand factor

Noncovalent binding energy generated between wild-type GPIba and VWF was -1096.7 ± 137.6 kcal/mol (▶Fig. 3, ▶Table 1). The noncovalent binding energy generated between G233A and G233V mutant GPIba with VWF were -929.8 ± 88.5 kcal/mol and -989.9 ± 94.0 kcal/mol, respectively. Both were 15.3 and 9.7% lower than that generated in

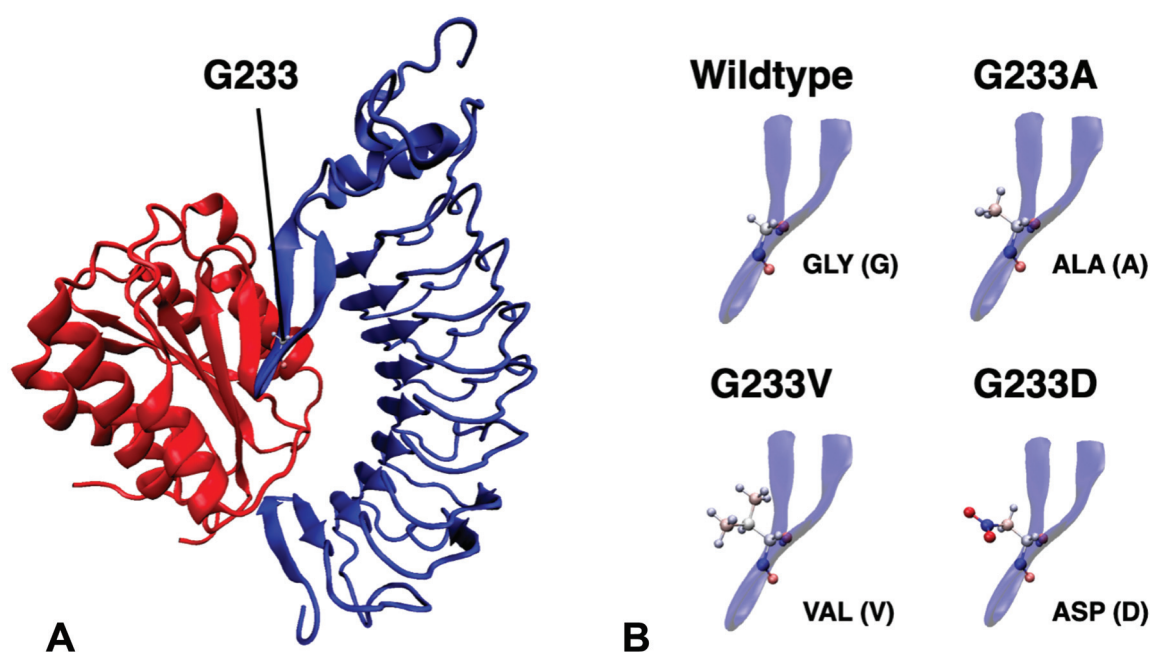


Fig. 1 Initial structure of VWF and GPIba in wild-type and the three mutants at G233. Panel A shows the position of G233 in N-terminus domain of GPIba (blue) binding with A1 domain of VWF (red). The initial positions of amino acid at 233 in wild-type (G) and the three mutants of G233A, G233V, and G233D are shown in panel B. The negatively charged carboxylate are shown in red, while the positively charged ammonium and guanidinium are shown in blue.

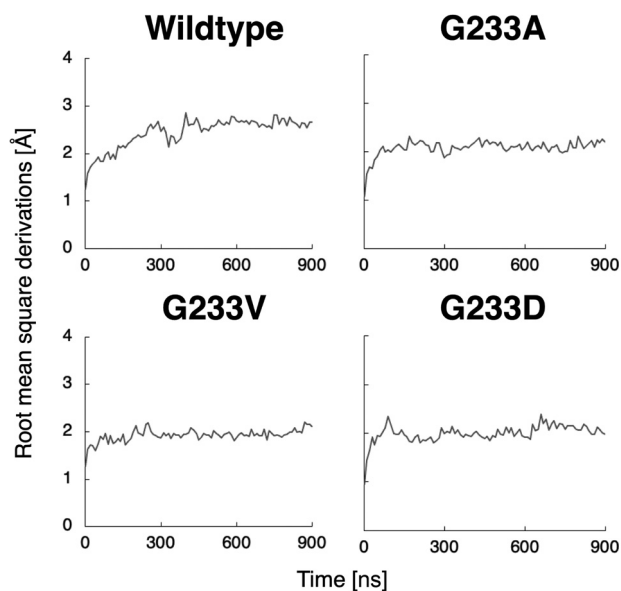


Fig. 2 Time-dependent changes in the root mean square deviations (RMSDs) of atoms constructing VWF and GPIba. The RMSDs of atoms constructing VWF and GPIba, excluding water molecules were calculated every 10 ns are shown in wild-type (left upper panel), G233A (right upper panel), G233V (left lower panel), and G233D (right lower panel).

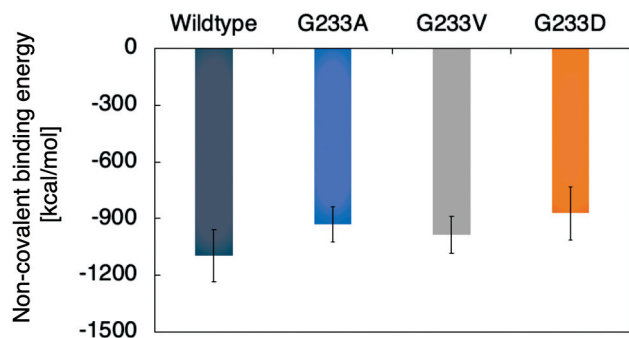


Fig. 3 Noncovalent binding energy generated between VWF and wild type, G233A, G233V, and G233D mutant of GPIba. The means and standard deviations of noncovalent binding energy generated between VWF and GPIba at wild-type (dark purple), G233A (light blue), G233V (gray), and G233D (orange) are shown in kcal/mol.

Table 1 Noncovalent binding energy generated between VWF and GPIba in wild-type and three of the mutants

Mutation	Noncovalent binding energy [kcal/mol]			p-Value
Wild-type	−1096.0	±	137.6	—
G233A	−929.8	±	88.5	<0.001
G233V	−989.9	±	94.0	<0.001

wild-type GPIba binding with VWF, respectively ($p < 0.001$ for both). For G233D mutant, the noncovalent binding energy generated between GPIba and VWF was -865.0 ± 139.1

kcal/mol which is 21.1% lower than the value in wild-type GPIba binding with VWF ($p < 0.001$). Time-dependent changes in noncovalent binding energy in all conditions did not differ substantially (►Supplemental Fig. S1).

Salt Bridge Formation between Amino Acids in Glycoprotein Iba and von Willebrand factor

Each panel of ►Fig. 4 shows the percentages of time periods when each pair of salt bridge was formed during the calculation period. ►Fig. 5 shows the results with a heat map. Six pairs of salt bridges (D63-R571, D83-K569, D106-K569, K237-D570, E14-R611, and E128-K608) were formed for more than 50% of the calculation period in wild-type GPIba binding with VWF. The distributions of time periods where various sets of salt bridges formed between each set of amino acids differ substantially among VWF binding with wild-type and the three G233 mutants of GPIba as shown in ►Figs. 4 and 5. The numbers of salt bridges formed for more than 50% of the time period in G233A-GPIba with VWF, G233V-GPIba with VWF, and G233D-GPIba with VWF were 6, 5, and 4, respectively. In a sensitivity analysis, the number of salt bridges formed was 8 in wild-type GPIba binding with VWF when the cut-off value was set as 40% as shown in ►Fig. 5. In this condition, number of salt bridges formed more than 40% of calculating period in VWF binding with G233A, V, and D mutants were 6, 7, and 5, respectively. Dynamic structural fluctuation around these salts bridge during the calculation period in each case is shown in ►Supplemental Movies S1 to S4.

Supplemental Movie S1

Results of MD calculations of VWF bound with wild-type GPIba. The snap shots of VWF (red) binding with GPIba (blue) calculated as the position coordinates in each 10 ns were reconstructed as the 90 frames movie. The amino acids forming salt bridges for more than 50 were shown as the Corey–Pauling–Koltun model (red in VWF and blue in GPIba). Online content including video sequences viewable at: <https://www.thieme-connect.com/products/ejournals/html/10.1055/a-1937-9940>.

Supplemental Movie S2

Results of MD calculations of VWF bound with G233A GPIba. The snap shots of VWF (red) binding with GPIba (blue) calculated as the position coordinates in each 10 ns were reconstructed as the 90 frames movie. The amino acids forming salt bridges for more than 50 were shown as the Corey–Pauling–Koltun model (red in VWF and blue in GPIba). Online content including video sequences viewable at: <https://www.thieme-connect.com/products/ejournals/html/10.1055/a-1937-9940>.

Supplemental Movie S3

Results of MD calculations of VWF bound with G233V GPIba. The snap shots of VWF (red) binding with GPIba (blue) calculated as the position coordinates in each 10 ns were reconstructed as the 90 frames movie. The amino acids forming salt bridges for more than 50 were shown as the Corey–Pauling–Koltun model (red in VWF and blue in GPIba). Online content including video sequences viewable at: <https://www.thieme-connect.com/products/ejournals/html/10.1055/a-1937-9940>.

Supplemental Movie S4

Results of MD calculations of VWF bound with G233D GPIba. The snap shots of VWF (red) binding with GPIba (blue) calculated as the position coordinates in each 10 ns were reconstructed as the 90 frames movie. The amino acids forming salt bridges for more than 50 were shown as the Corey–Pauling–Koltun model (red in VWF and blue in GPIba). Online content including video sequences viewable at: <https://www.thieme-connect.com/products/ejournals/html/10.1055/a-1937-9940>.

GPIba-VWF	wildtype	G233A	G233V	G233D
E5-K549	32	14	49	5
E14-K549	3	0	0	11
E14-R552	5	88	3	22
E14-R611	50	1	93	5
D18-K549	41	0	7	12
E40-R573	45	0	82	0
D63-R571	80	100	97	100
D83-K569	100	27	24	15
D106-K569	99	4	24	2
E128-K608	73	86	0	88
E151-K644	0	7	0	1
E225-R629	0	5	4	15
E225-R632	29	51	47	43
D235-K572	29	84	70	66
D235-R579	27	1	2	8
K237-D570	82	51	91	71

Fig. 5 Probability of the presence of salt bridges formed between VWF and GPIba. The probabilities of the presence of each pair of amino acid forming salt bridge are shown in the heat map. The pair of salt bridge formation more than 50% of calculation periods were shown with the color including red. The number of salt bridge formed more than 50% is apparently higher in wild-type and G233V mutant with VWF. The number of salt bridges is substantially lower in G233D mutant.

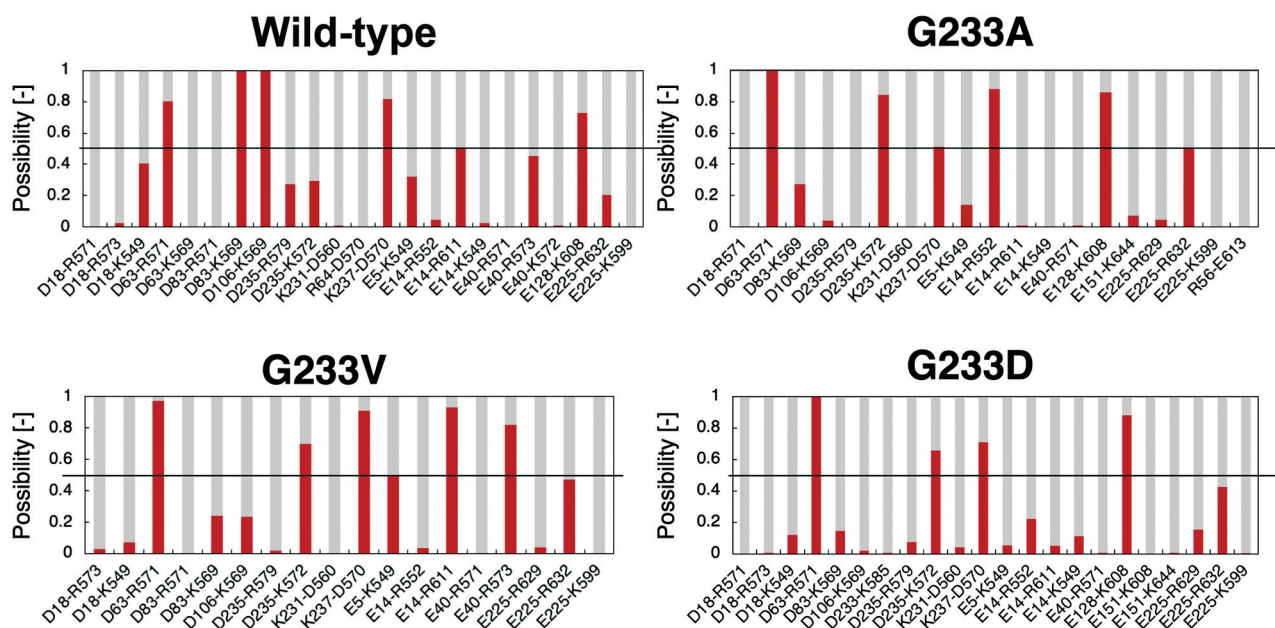


Fig. 4 Probability of the presence of salt bridges formed between VWF and GPIba. The probabilities of salt bridge formation for the pairs of amino acids in GPIba-VWF shown at the bottom of each panel are shown in red bar. The upper left panel shows the results of VWF binding with wild-type GPIba. The upper right, lower left, and lower right panel show the results of VWF binding with G233A, G233V, and G233D mutants of GPIba, respectively. Thin black line in each panel shows the threshold of 50%.

Discussion

Our MD simulation showed that the specific physical characteristics of the probability of salt bridge formation were lower in VWF binding to G233D mutant of GPIba generating less noncovalent binding energy as compared with the binding to GPIba in wild-type, G233A, and G233V mutants. So far, the quantitative relationships between the physical parameters of molecules such as noncovalent binding energy between VWF and GPIba, and their biological functions are still to be clarified. Our finding supporting lower probabilities of salt bridge formation with less noncovalent binding energy in biological loss of function mutation in G233D is in agreement with the hypothesis that the biological functions of macromolecules could be influenced by small changes in their physiological characteristics.⁴⁴ Indeed, the loss of VWF binding function in G233D mutant in GPIba was associated with only 21.1% reductions in noncovalent binding energy with only slightly low probabilities of salt bridge formation between them.

One important and specific characteristic of VWF binding with GPIba is that their binding could be detected only under shear flow conditions or in the presence of specific modulators of ristocetin or botrocetin unless with a specific gain of function mutants.^{4,15,18,45,46} Our MD simulation was conducted in the absence of any modulators. Thus, our results represent the conditions of transient VWF binding with GPIba under shear flow conditions. Our results suggest that the loss of VWF binding function in G233D GPIba under shear flow condition²³ is caused by a small change in the probabilities of salt bridge formation and slightly lower noncovalent binding energy between GPIba and VWF.

Despite numerous attempts,^{15,19,47–49} an assay system accurately quantifying physical parameters of VWF binding with GPIba under shear flow conditions has not been established. MD simulation enabled to quantify the physical parameters of VWF binding with GPIba in wild-type and three G233 mutants. The quantitative physical parameters obtained by our MD simulation such as noncovalent binding energy in VWF and GPIba provide a clue to understanding the biological function of GPIba and VWF in the absence of specific modulators where the bindings are transient.

The lowest numbers of salt bridge formations and lowest noncovalent binding energy in VWF binding with the loss of function G233D mutant of GPIba as compared with wild-type, equal of function (G233A), and gain of function mutant (G233V) may suggest both the salt bridges and noncovalent binding energy did not reach the threshold necessary to keep the bond between the two molecules strong enough to resist against the fluid shear force. Our results are in agreement with the idea that biological characteristics of protein–protein interaction such as binding depend on the threshold of the probabilities in salt bridge formation and the noncovalent binding energy in them. Yet, the quantitative relationship between physical characteristics of protein bonds and their biological function is still to be elucidated.

Phenotype of the “loss of function” mutants results in a higher risk of bleeding. It is interesting that the bleeding risks

were also increased in the “gain of function” mutants. Higher bleeding risk in “gain of function” mutants was explained by the consumption of larger multimers of VWF by their binding with platelets.^{22,50} Our MD calculation did not provide a direct clue to explain the behavior of the “gain of function mutant” of G233V by the number of salt bridges or noncovalent binding energy. It is of note that our MD calculation was started from the structure of VWF bound with GPIba in an energetically stable manner. The structural characteristic of VWF bound with GPIba may differ substantially under the condition where external forces generated by blood flow to the platelet are applied to these molecules.⁵¹ Moreover, the focus of our simulation calculations is to quantify the physical parameters of molecules at nanometer scale (10^{-9} meter) from the physical behaviors of atomic at Å scale (10^{-10} meter). The clinical events of bleeding occur in organ at a millimeter scale (10^{-3} meter). Our MD simulation results are helpful to understand the binding functions of VWF and GPIba at the molecule level but hard to apply directly to dissect the mechanism of the increased risk of bleeding in G233 mutants.

MD calculations provide precise dynamic structures and their physical parameters of target protein even in the presence of interaction with other proteins by calculation with the fundamental law of simple Newton's equation. There is a potential methodological limitation to obtain physical parameters of target molecules from the sum of Newton's equation because the physical movements of atoms sharing electrical cloud should follow the probability-dependent quantum mechanics. In our calculations, quantum mechanics were coarse grained into molecular mechanics by using the CHARMM force field.^{52,53} Despite the fact that the validity of CHARMM force field has been confirmed in various macromolecules,^{52,54} coarse graining quantum mechanics into molecular mechanics may induce errors. So far, the biochemical characteristics of VWF binding with GPIba predicted by MD with CHARMM force field² were in agreements with the results from other biochemical experiments in a qualitative manner.^{55,56} The lower numbers of salt bridges and noncovalent binding energy in VWF binding with G233D mutant of GPIba are in agreements with qualitative biological function of G233D mutant. Our findings agree with the hypothesis that the biological functions of macromolecules could be influenced by small changes in their physiological parameters. The quantitative relationships between the calculated physical parameters of target protein interactions and their biological function are still to be elucidated.

In conclusion, our results showing lower probability of salt bridge formation with less noncovalent binding energy in loss of function mutant of G233D GPIba as compared with wild-type, G233A, and G233V in regard to the binding with VWF support the notion that the biological functions of macromolecules could be influenced by only small changes in their physiological parameters. Further investigations are necessary to dissect the mechanism of the gain of function achieve by G233V mutation.

What is Known About This Topic?

- Platelet glycoprotein (GP) Iba binding with the A1 domain of von Willebrand factor (VWF) plays a crucial role in platelet adhesion under the high wall shear stress condition.
- A single amino acid mutation at residue 233 of platelet glycoprotein (GP) Iba from glycine (G) to alanine (A), aspartic acid (D), and valine (V) results in equal, loss, and gain of function, respectively, for the binding with VWF.
- The analysis of potential of mean force (PMF) revealed that the dissociation energy for VWF binding with GPIba was 4.32 kcal/mol (19.5%) lower in VWF binding with G233D mutant than that with the wild-type.

What does This Paper Add?

- There were six salt bridges detected for more than 50% of the calculation period in wild-type GPIba binding with A1 domain of VWF generating a noncovalent binding energy of -1096 ± 137.6 kcal/mol.
- Only four pairs of salt bridges with noncovalent binding energy of -865 ± 139 were present for over 50% of the calculation period in G233D GPIba binding with VWF.
- There were six and five pairs of salt bridges generating -929.8 ± 88.5 and -989.9 ± 94.0 kcal/mol of noncovalent binding energy in G233A and G233V mutant-GPIba binding with VWF.
- The biological loss of function of G233D mutant-GPIba binding with VWF was associated with the physical characteristics of slightly less probability of salt bridge formation with slightly lower noncovalent binding energy in their binding.

Funding

The authors acknowledged funding from grant-in-aid for MEXT/JSPS KAKENHI 19H03661, AMED grant number A368TS, A447TR, Bristol-Myers Squibb for an independent research support project (33999603) and a grant from Nakatani Foundation for Advancement of Measuring Technologies in Biomedical Engineering and Vehicle Racing Commemorative Foundation (6236). The author S.G. acknowledged partial financial support from Sanofi, Pfizer, Bristol Myer Squibb, and Ono Pharma.

Conflict of Interests

The author S.G. acknowledged receiving a consultation fee from Anthos Therapeutics, and Janssen Pharmaceutical, and also personal fee from Duke University as a member of the Steering Committee for EMPACT-MI trial. The author S.G. and M.N. have nothing to disclose.

References

- Deng W, Wang Y, Druzak SA, et al. A discontinuous autoinhibitory module masks the A1 domain of von Willebrand factor. *J Thromb Haemost* 2017;15(09):1867–1877
- Shiozaki S, Takagi S, Goto S. Prediction of molecular interaction between platelet glycoprotein Iba and von Willebrand factor using molecular dynamics simulations. *J Atheroscler Thromb* 2016;23(04):455–464
- Emsley J, Cruz M, Handin R, Liddington R. Crystal structure of the von Willebrand Factor A1 domain and implications for the binding of platelet glycoprotein Ib. *J Biol Chem* 1998;273(17):10396–10401
- Savage B, Saldívar E, Ruggeri ZM. Initiation of platelet adhesion by arrest onto fibrinogen or translocation on von Willebrand factor. *Cell* 1996;84(02):289–297
- Goto S, Ikeda Y, Saldívar E, Ruggeri ZM. Distinct mechanisms of platelet aggregation as a consequence of different shearing flow conditions. *J Clin Invest* 1998;101(02):479–486
- Quach ME, Li R. Structure-function of platelet glycoprotein Ib-IX. *J Thromb Haemost* 2020;18(12):3131–3141
- Kulkarni S, Dopheide SM, Yap CL, et al. A revised model of platelet aggregation. *J Clin Invest* 2000;105(06):783–791
- Jordan D. Ristocetin. In *Mechanism of Action*. Berlin, Heidelberg: Springer; 1967:84–89
- Howard MA, Firkin BG. Ristocetin—a new tool in the investigation of platelet aggregation. *Thromb Diath Haemorrh* 1971;26(02):362–369
- Andrews RK, Booth WJ, Gorman JJ, Castaldi PA, Berndt MC. Purification of botrocetin from Bothrops jararaca venom. Analysis of the botrocetin-mediated interaction between von Willebrand factor and the human platelet membrane glycoprotein Ib-IX complex. *Biochemistry* 1989;28(21):8317–8326
- Coller BS, Peerschke EI, Scudder LE, Sullivan CA. Studies with a murine monoclonal antibody that abolishes ristocetin-induced binding of von Willebrand factor to platelets: additional evidence in support of GPIb as a platelet receptor for von Willebrand factor. *Blood* 1983;61(01):99–110
- Read MS, Smith SV, Lamb MA, Brinkhous KM. Role of botrocetin in platelet agglutination: formation of an activated complex of botrocetin and von Willebrand factor. *Blood* 1989;74(03):1031–1035
- Sen U, Vasudevan S, Subbarao G, et al. Crystal structure of the von Willebrand factor modulator botrocetin. *Biochemistry* 2001;40(02):345–352
- Calvete JJ. Platelet integrin GPIIb/IIIa: structure-function correlations. An update and lessons from other integrins. *Proc Soc Exp Biol Med* 1999;222(01):29–38
- Goto S, Salomon DR, Ikeda Y, Ruggeri ZM. Characterization of the unique mechanism mediating the shear-dependent binding of soluble von Willebrand factor to platelets. *J Biol Chem* 1995;270(40):23352–23361
- Goto S. Role of von Willebrand factor for the onset of arterial thrombosis. *Clin Lab* 2001;47(7-8):327–334
- Sadler JE, Budde U, Eikenboom JC, et al; Working Party on von Willebrand Disease Classification. Update on the pathophysiology and classification of von Willebrand disease: a report of the Subcommittee on von Willebrand Factor. *J Thromb Haemost* 2006;4(10):2103–2114
- Savage B, Almus-Jacobs F, Ruggeri ZM. Specific synergy of multiple substrate-receptor interactions in platelet thrombus formation under flow. *Cell* 1998;94(05):657–666
- Ikeda Y, Handa M, Kawano K, et al. The role of von Willebrand factor and fibrinogen in platelet aggregation under varying shear stress. *J Clin Invest* 1991;87(04):1234–1240
- Othman M, Kaur H, Emsley J. Platelet-type von Willebrand disease: new insights into the molecular pathophysiology of a unique platelet defect. *Semin Thromb Hemost* 2013;39(06):663–673

- 21 Miller JL, Castella A. Platelet-type von Willebrand's disease: characterization of a new bleeding disorder. *Blood* 1982;60(03):790–794
- 22 Sadler JEF. For the Subcommittee on von Willebrand Factor of the Scientific and Standardization Committee of the International Society on Thrombosis and Haemostasis. A revised classification of von Willebrand disease. *Thromb Haemost* 1994;71(04):520–525
- 23 Matsubara Y, Murata M, Sugita K, Ikeda Y. Identification of a novel point mutation in platelet glycoprotein Iba α , Gly to Ser at residue 233, in a Japanese family with platelet-type von Willebrand disease. *J Thromb Haemost* 2003;1(10):2198–2205
- 24 Hulstein JJJ, de Groot PG, Silence K, Veyradier A, Fijnheer R, Lenting PJ. A novel nanobody that detects the gain-of-function phenotype of von Willebrand factor in ADAMTS13 deficiency and von Willebrand disease type 2B. *Blood* 2005;106(09):3035–3042
- 25 Dong J, Schade AJ, Romo GM, et al. Novel gain-of-function mutations of platelet glycoprotein Iba α by valine mutagenesis in the Cys209–Cys248 disulfide loop. Functional analysis under static and dynamic conditions. *J Biol Chem* 2000;275(36):27663–27670
- 26 Tait AS, Cranmer SL, Jackson SP, Dawes IW, Chong BH. Phenotype changes resulting in high-affinity binding of von Willebrand factor to recombinant glycoprotein Ib-IX: analysis of the platelet-type von Willebrand disease mutations. *Blood* 2001;98(06):1812–1818
- 27 Huizinga EG, Tsuji S, Romijn RA, et al. Structures of glycoprotein Iba α and its complex with von Willebrand factor A1 domain. *Science* 2002;297(5584):1176–1179
- 28 Miller JL, Cunningham D, Lyle VA, Finch CN. Mutation in the gene encoding the alpha chain of platelet glycoprotein Ib in platelet-type von Willebrand disease. *Proc Natl Acad Sci U S A* 1991;88(11):4761–4765
- 29 Russell SD, Roth GJ. Pseudo-von Willebrand disease: a mutation in the platelet glycoprotein Ib alpha gene associated with a hyperactive surface receptor. *Blood* 1993;81(07):1787–1791
- 30 Lin J, Seeman NC, Vaidehi N. Molecular-dynamics simulations of insertion of chemically modified DNA nanostructures into a water-chloroform interface. *Biophys J* 2008;95(03):1099–1107
- 31 Goto S, Oka H, Ayabe K, et al. Prediction of binding characteristics between von Willebrand factor and platelet glycoprotein Iba α with various mutations by molecular dynamic simulation. *Thromb Res* 2019;184:129–135
- 32 Interlandi G, Yakovenko O, Tu A-Y, et al. Specific electrostatic interactions between charged amino acid residues regulate binding of von Willebrand factor to blood platelets. *J Biol Chem* 2017;292(45):18608–18617
- 33 Boonstra S, Onck PR, Giessen Ev. CHARMM TIP3P water model suppresses peptide folding by solvating the unfolded state. *J Phys Chem B* 2016;120(15):3692–3698
- 34 Wang L, O'Mara ML. Effect of the force field on molecular dynamics simulations of the multidrug efflux protein P-glycoprotein. *J Chem Theory Comput* 2021;17(10):6491–6508
- 35 Janowski PA, Liu C, Deckman J, Case DA. Molecular dynamics simulation of trypsin lysozyme in a crystal lattice. *Protein Sci* 2016;25(01):87–102
- 36 Cerný J, Hobza P. Non-covalent interactions in biomacromolecules. *Phys Chem Phys* 2007;9(39):5291–5303
- 37 Eskici G, Axelsen PH. Amyloid beta peptide folding in reverse micelles. *J Am Chem Soc* 2017;139(28):9566–9575
- 38 Humphrey W, Dalke A, Schulten K. VMD: visual molecular dynamics. *J Mol Graph* 1996;14(01):33–38, 27–28
- 39 Kakiuchi T. Salt bridge in electroanalytical chemistry: past, present, and future. *J Solid State Electrochem* 2011;15:1661–1671. Doi: 10.1007/s10008-011-1373-0
- 40 Bosshard HR, Marti DN, Jelesarov I. Protein stabilization by salt bridges: concepts, experimental approaches and clarification of some misunderstandings. *J Mol Recognit* 2004;17(01):1–16
- 41 Kumar S, Nussinov R. Close-range electrostatic interactions in proteins. *ChemBioChem* 2002;3(07):604–617
- 42 Ahmed MC, Papaleo E, Lindorff-Larsen K. How well do force fields capture the strength of salt bridges in proteins? *PeerJ* 2018;6:e4967
- 43 Interlandi G, Thomas W. The catch bond mechanism between von Willebrand factor and platelet surface receptors investigated by molecular dynamics simulations. *Proteins* 2010;78(11):2506–2522
- 44 Krissinel E, Henrick K. Inference of macromolecular assemblies from crystalline state. *J Mol Biol* 2007;372(03):774–797
- 45 Dong J-F, Berndt MC, Schade A, McIntire LV, Andrews RK, López JA. Ristocetin-dependent, but not botrocetin-dependent, binding of von Willebrand factor to the platelet glycoprotein Ib-IX-V complex correlates with shear-dependent interactions. *Blood* 2001;97(01):162–168
- 46 Hillery CA, Mancuso DJ, Evan Sadler J, et al. Type 2M von Willebrand disease: F606I and I662F mutations in the glycoprotein Ib binding domain selectively impair ristocetin- but not botrocetin-mediated binding of von Willebrand factor to platelets. *Blood* 1998;91(05):1572–1581
- 47 Moake JL, Turner NA, Stathopoulos NA, Nolasco L, Hellums JD. Shear-induced platelet aggregation can be mediated by vWF released from platelets, as well as by exogenous large or unusually large vWF multimers, requires adenosine diphosphate, and is resistant to aspirin. *Blood* 1988;71(05):1366–1374
- 48 Goto S, Sakai H, Goto M, et al. Enhanced shear-induced platelet aggregation in acute myocardial infarction. *Circulation* 1999;99(05):608–613
- 49 Goto S, Tamura N, Eto K, Ikeda Y, Handa S. Functional significance of adenosine 5'-diphosphate receptor (P2Y₁₂) in platelet activation initiated by binding of von Willebrand factor to platelet GP Iba α induced by conditions of high shear rate. *Circulation* 2002;105(21):2531–2536f
- 50 Othman M. Platelet-type Von Willebrand disease: three decades in the life of a rare bleeding disorder. *Blood Rev* 2011;25(04):147–153
- 51 Tamura N, Shimizu K, Shiozaki S, et al. Important regulatory roles of erythrocytes in platelet adhesion to the von Willebrand factor on the wall under blood flow conditions. *Thromb Haemost* 2022;122(06):974–983
- 52 Schmidt JM, Brueschweiler R, Ernst RR, et al. Molecular dynamics simulation of the proline conformational equilibrium and dynamics in antamanide using the CHARMM force field. *J Am Chem Soc* 1993;115:8747–8756
- 53 Lagant P, Nolde D, Stote R, et al. Increasing normal modes analysis accuracy: The SPASIBA spectroscopic force field introduced into the CHARMM program. *J Phys Chem A* 2004;108:4019–4029
- 54 Brooks BR, Brooks CL III, Mackerell AD Jr, et al. CHARMM: the biomolecular simulation program. *J Comput Chem* 2009;30(10):1545–1614
- 55 Tobimatsu H, Nishibuchi Y, Sudo R, Goto S, Tanishita K. Adhesive forces between A1 domain of von Willebrand factor and N-terminus domain of glycoprotein Iba α measured by atomic force microscopy. *J Atheroscler Thromb* 2015;22(10):1091–1099
- 56 Kim J, Zhang CZ, Zhang X, Springer TA. A mechanically stabilized receptor-ligand flex-bond important in the vasculature. *Nature* 2010;466(7309):992–995